Int J Adv Manuf Technol (2009) 44:80–90
DOI 10.1007/s00170-008-1799-4

ORIGINAL ARTICLE

Optimization of STM/FIM nanotip aspect ratio based on the Taguchi method

Gh. Tahmasebipour · Y. Hojjat · V. Ahmadi · A. Abdullah

Received: 3 May 2008 / Accepted: 9 October 2008 / Published online: 29 October 2008

Abstract This paper presents optimization of electrochemical etching parameters to achieve the optimum aspect ratio of the scanning tunneling microscopy/field ion microscopy tungsten nanotip by using Taguchi method. The combination of optimum level of process parameters was obtained by using the analysis of signal-to-noise ratio. The level of importance of the process parameters on the nanotip aspect ratio was determined by using analysis of variance. It was found that the optimum level of process parameters are electrolyte concentration of 2 M/lit, wire immersion length of 2.5 mm, cathode tube inner diameter of 40 mm, and voltage of 3.5 V. Within the range of experiments and the process parameters in terms of impact significance were found to be electrolyte concentration, process voltage, wire immersion length, and inner diameter of cathode tube, respectively. By using the optimum level of the process parameters, the nanotip aspect ratio was enhanced by 263% in comparison to the mean value of the experimental results. The nanotip aspect ratio of up to 163:1 was obtained in the present research.

Keywords Nanotip optimization · Tip aspect ratio · Electrochemical etching · Taguchi method · Scanning tunneling microscopy (STM) · Field ion microscopy (FIM)

G. Tahmasebipour · Y. Hojjat
Mechanical Engineering Department, Tarbiat Modares University, Tehran, Iran

V. Ahmadi
Electrical Engineering Department, Tarbiat Modares University, Tehran, Iran

A. Abdullah (✉)
Mechanical Engineering Department,
Amirkabir University of Technology,
Tehran, Iran
e-mail: amirah@aut.ac.ir

1 Introduction

During past decades, development of electron microscopy, field ion microscopy (FIM), and scanning tunneling microscopy (STM) has driven the development of sharp metallic tips as a main part of these microscopes. Increase of aspect ratio (ratio of nanometric apex tip length to tip radius) of FIM tip results in uniformity and stability of the field emitted current [1], and consequently, it improves readability and reliability of FIM images. Larger aspect ratio of STM tip leads to improvement of reliability of STM images too, especially in imaging of nanometric deep trenches [2, 3] and rough profiles [4]. Influence of tip aspect ratio on STM image readability and reliability is shown in Fig. 1.

Electrochemical etching is the most practical method for fabrication of nanotips with desired quality, reproducibility, and high reliability [5]. The material used for fabrication of the tips is normally tungsten, platinum, platinum–iridium, gold, and silver [6]. A STM tip must have high electrical conductivity, high mechanical strength, and high durability. Tip strength prevents deformation of tip during imaging, and it can cause generation of images with high repeatability and reliability. When the aspect ratio of the tip apex is high, its mechanical strength and durability becomes more important. For this reason, with the exception of particular applications, tungsten is the first choice for fabrication of STM tip and most of the researchers have concentrated on this material [7–14].

For fabrication of STM/FIM nanotips, several researchers [7–24] have studied electrochemical etching and some of its related aspects. The most important parameters that govern the nanotip fabrication process are the time delay in turning off the voltage at the end of tip fabrication process, the electrolyte concentration, immersion length of the wire,

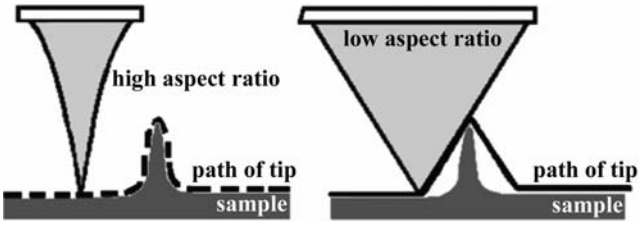

Fig. 1 Influence of tip aspect ratio on STM image readability and reliability

inner diameter of the cathode tube, and the process voltage. The closest research to the present effort is from Krakauer et al. They used micropulse voltage source for reducing the time delay in turning off the voltage at the end of tip fabrication process [25, 26]. Decrease of this time delay and its influence on the tip sharpness have been the subject of researches through design and fabrication of different electronic circuits [9, 27, 28]. An improved feedback control technique for fabrication of scanning tunneling microscopy tips by direct current (DC) electrochemical process was presented by Anwei et al. Distinguished from the conventional control techniques, etching current was directly used as the only control signal by comparing it with the reference current [29]. In the present work, an electronic control circuit was designed and implemented for monitoring the process automatically and turning off the voltage within 100 ns.

For improvement of tip surface smoothness, Xu et al. used a constant voltage, with the wire immersed below the nominal air/electrolyte interface by no more than one half of the wire diameter and stopping the etching at different current levels. This process provided a tip radius range of approximately 100 nm to 5 μm and the surface roughness of about 0.3 nm root mean square for a tungsten wire with 0.2 mm diameter [30]. In the present study, tungsten wire diameter of 0.3 mm and wire immersion length of 2.5 to 7 mm was used and the nanotip apex radius of 15 to 80 nm was obtained.

In researches carried out by Kerfriden et al., it was observed that the length of the lower part of immersed tungsten wire within the range of 10 to 100 mm did not have a significant effect on the characteristics of the apex of the upper part of the wire [7]. To extend the domain of investigations, in the present research, the range of wire immersion length was selected between 2.5 to 7 mm, and it was observed that the length of the lower part of the wire less than 7 mm has significant effect on the nanotip aspect ratio.

Kim et al. investigated the effects of the magnitude of an attached mass at the end of the immersed wire on the tip shape. In addition, the variation of tip shape with respect to the shape of applied constant or pulsed voltage was examined. The yield rate of the tips was increased up to around 60% with the attached mass method [31]. In the present study, the weight of the various immersion lengths of the wire was used as a control parameter and the optimum immersion length was obtained to earn higher nanotip aspect ratio.

The nanotips with the aspect ratio greater than 3:1 (tip length/diameter) or 6:1 (tip length/radius) are counted as high aspect ratio nanotips [32]. The STM/FIM nanotip aspect ratio of 11:1 to 81.5:1 (22:1–163:1 nanotip length/radius) was obtained in this study. The nanotip aspect ratio was enhanced by 263% in comparison to the mean value of the experimental results by using the optimum level of the process parameters.

To author's knowledge, in spite of wide use of electrochemically etched tungsten nanotips in STM/FIM based researches, effects of electrochemical etching parameters such as the electrolyte concentration, immersion length of the wire, inner diameter of the cathode tube, and the process voltage on the STM/FIM nanotip aspect ratio have not yet been extensively studied. In this research work, by studying the effects of these parameters on the STM/FIM nanotip aspect ratio, the Taguchi method was used for determining the optimum level of nanotip fabrication parameters and their priority for achieving optimum aspect ratio.

In the next section, experimental procedure will be discussed. Section 3 contains process optimization by employing Taguchi method. Section 4 has been dedicated to analysis of experimental results and discussion. Confirmation experiment will be discussed in Section 5 and finally the concluding remarks will be given in Section 6.

2 Experimental procedure

The nanotip fabrication method used in this research was electrochemical etching process. In this process, a small

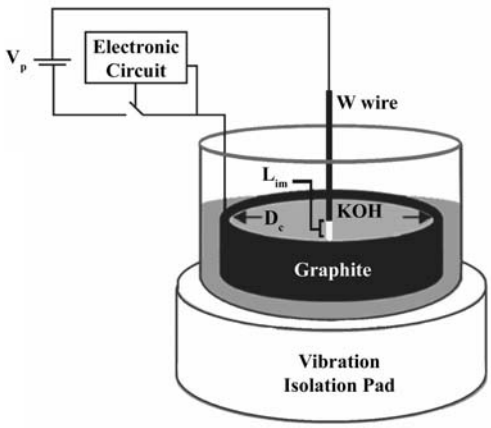

Fig. 2 Schematic diagram of experimental setup; wall thickness and height of graphite ring (also, height of electrolyte) are 8 and 20 mm, respectively

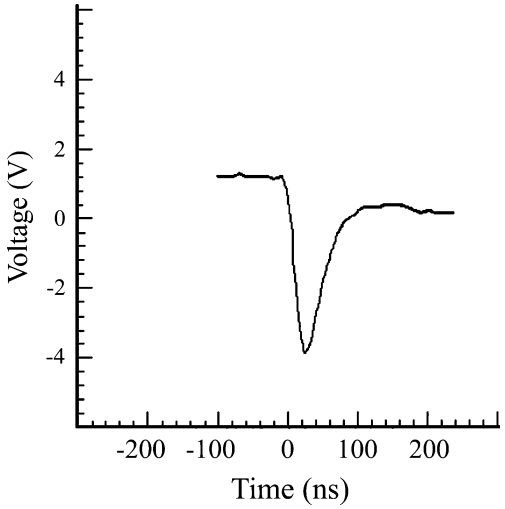

Fig. 3 Time delay diagram of turning off the voltage

diameter (0.3 mm) tungsten wire was dipped into an electrolyte solution inside a graphite tube and the voltage was applied across the wire and the tube. The most common electrolytes used for electrochemical etching of tungsten are KOH and NaOH [12, 13, 33]. In this research, solution of KOH in deionized water was used. Figure 2 shows schematic diagram of experimental setup for nanotip fabrication. V_p, L_{im}, and D_c are process voltage, wire immersion length, and inner diameter of the cathode tube, respectively.

When tungsten wire is immersed into the electrolyte, the capillary forces yield formation of a meniscus of electrolyte around the wire. At the top of meniscus, the rate of etching is almost nil and the etching rate increases from the top to the skirt. This can be explained by the variation of electrolyte volume along the meniscus. On the other hand, the soluble tungstate produced during the reaction flows down towards the lower end of the wire, generating a dense viscous layer that prevents this region from being etched away. Thus, a necking phenomenon is observed on the stem of the wire at the bottom of the meniscus. This part of the wire becomes so thin that its tensile strength cannot sustain the weight of the lower end of the wire. The latter one breaks off and a very sharp tip is left behind. At this moment, if the applied voltage is not turned off, the tip apex starts to be etched and its aspect ratio and sharpness will decrease [14, 17, 22, 23]. Some researchers conducted investigations on decrease of time delay in turning off the voltage and the effects of this delay on the tip sharpness by designing and construction of various electronic circuits [9, 25–28]. In this work, an electronic circuit was designed and fabricated which could automatically monitor the process and turn off the voltage with a delay of 100 ns. Figure 3 shows the speed of this electronic circuit in turning of the process voltage.

3 Process optimization by using Taguchi method

Taguchi method [34–38] is a quite effective way to deal with responses dependent upon multivariables. This method is a powerful tool for design of experiments and provides a simple, efficient, and systematic approach to determine optimum process parameters. Compared with the conventional approach, this method reduces drastically the number of experiments that are required to model the response functions. Traditional experimentation involves variation of one-factor-at-a-time method, wherein the rest are held constant. For studying the individual effects of all factors, a lot of time and money must be spent. Taguchi technique overcomes all these drawbacks. In this method, the main effect is defined as the average value of the response function at a particular level of a parameter. The effect of a factor level is the deviation it causes from the overall mean response. The Taguchi method was devised for process optimization and identification of optimum combinations of factors for given responses. The steps involved in the Taguchi method are depicted as follows:

1. Identifying the main functions and the process parameters to be evaluated
2. Determination of the number of levels for the process parameters
3. Selecting the appropriate orthogonal array and assigning the process parameters to the orthogonal array and conducting the experiments accordingly

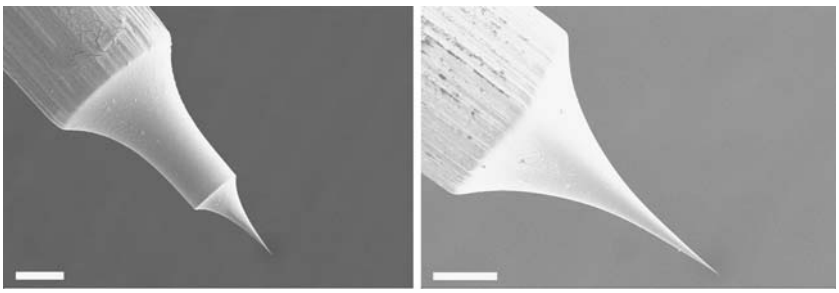

Fig. 4 Two samples of fabricated tungsten nanotips with DC voltage (the *white scale bar* in each subfigure is equal to 100 μm)

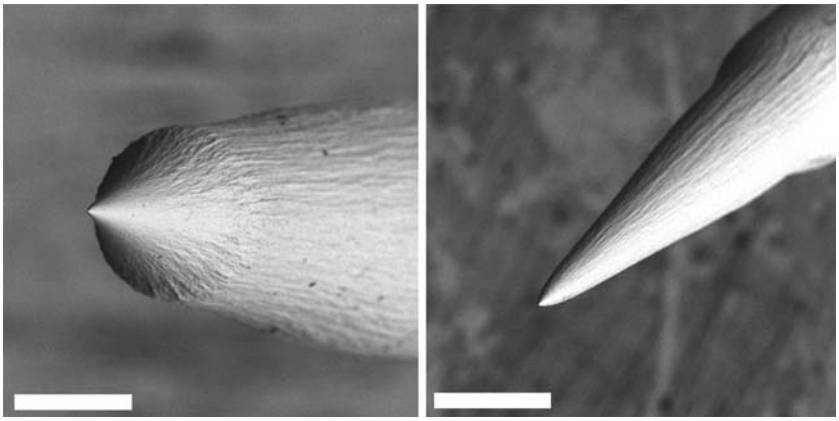

Fig. 5 Two samples of fabricated tungsten nanotips with AC voltage (the *white scale bar* in each subfigure is equal to 200 μm)

4. Studying the experimental results by analysis of signal-to-noise (S/N) ratios to determine the optimum level of process parameters
5. Investigating the results by analysis of variance (ANOVA) to identify the significance level of the process parameters on the main function
6. Verifying the optimum process parameters through a confirmation experiment

In this research, aspect ratio of the nanotip apex was taken as the main function of the nanotip fabrication process. Aspect ratio is defined as the nanometric apex tip length divided by tip radius. The most important influencing parameters on this ratio are the time delay in turning off the process voltage, electrolyte concentration (E_c), immersion length of the tungsten wire (L_{im}), inner diameter of the cathode tube (D_c), and the process voltage (V_p). No evidence was found to demonstrate the influence of these parameters on the nanotip aspect ratio. Therefore, based on the team experiences, these parameters were selected as E_c, in the range of 1 to 4 M/lit; L_{im}, 2.5 to 7 mm; D_c 40 to 110 mm; and V_p of DC voltage in the range of 2 to 3.5 V.

As already mentioned, with design and fabrication of an electronic circuit, the time delay in turning off the process voltage was fixed on 100 ns. Some experiments were conducted to understand the effects of voltage type (alternating current (AC)/DC) on the nanotip apex. It was found that the nanotips fabricated under DC voltage have apex of hyperbolic shape with high aspect ratio while the nanotips fabricated under AC voltage have conic form apex with low aspect ratio as it is shown in Figs. 4 and 5, respectively. As a result, DC voltage was selected for the nanotip fabrication process. Minimum voltage for initiation of tungsten electrochemical dissolution with KOH electrolyte is 1.43 V [39]. On the other hand, using a voltage above 4 V causes growth of a thick oxide layer on the tip apex [17]. This prevents tunneling current in STM. Thus, V_p range was selected to be between 2 to 3.5 V.

Regarding Taguchi quality design concept, process parameters E_c, L_{im}, D_c, and V_p were defined in four levels

Table 1 L_{16} orthogonal array of experiments and their results (lowest value of input parameters coincide with lowest level of those parameters)

Experiment no.	E_c (M/lit)	L_{im} (mm)	D_c (mm)	V_p (V)	L_t (nm)	R_t (nm)	Aspect ratio (L_t/R_t)	S/N ratio (dB)
1	1	2.5	40	2	3,440	60	57	35.1175
2	1	4	55	2.5	1,100	50	22	26.8485
3	1	5.5	75	3	2,290	55	42	32.4650
4	1	7	110	3.5	2,345	45	52	34.3201
5	2	2.5	55	3.5	4,070	25	163	44.2438
6	2	4	40	3	4,365	35	125	41.9382
7	2	5.5	110	2.5	3,055	55	56	34.9638
8	2	7	75	2	5,750	50	115	41.2140
9	3	2.5	75	2.5	2,515	60	42	32.4650
10	3	4	110	2	1,900	65	29	29.2480
11	3	5.5	40	3.5	4,335	45	96	39.6454
12	3	7	55	3	6,430	60	107	40.5877
13	4	2.5	110	3	2,320	50	46	33.2552
14	4	4	75	3.5	1,215	35	35	30.8814
15	4	5.5	55	2	1,950	55	35	30.8814
16	4	7	40	2.5	2,030	80	25	27.9588

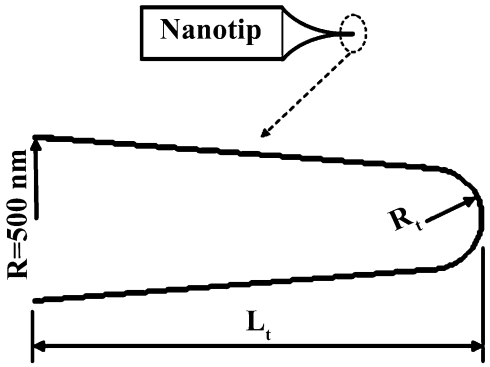

Fig. 6 Schematic form of the nanometric apex of tip

and an L_{16} orthogonal array table was chosen for the experiments as shown in Table 1. The experiments were conducted according to the selected orthogonal array.

Figure 6 shows schematic diagram of nanotip apex. R_t is the radius and L_t is the length of nanotip from apex to where the cross section radius equals to 500 nm. Scanning electron microscopy (SEM) images of apexes of fabricated nanotips were taken with magnifications of ×6–15K and ×50–200K as shown in Figs. 7 and 8, respectively. SEM images shown in Figs. 7 and 8 were used to measure L_t and R_t, respectively. The calculated values of the nanotips aspect ratio (L_t/R_t) are given in Table 1.

4 Experimental results analysis and discussion

4.1 Analysis of signal-to-noise ratio

Based on Taguchi method [34–38], optimum level of process parameters is determined by analysis of S/N ratio. There are several categories of performance characteristics in the analysis of the S/N ratio as lower is better, nominal is best, and higher is better (HB). Since the nanotip aspect ratio should be as high as possible, the HB was selected for

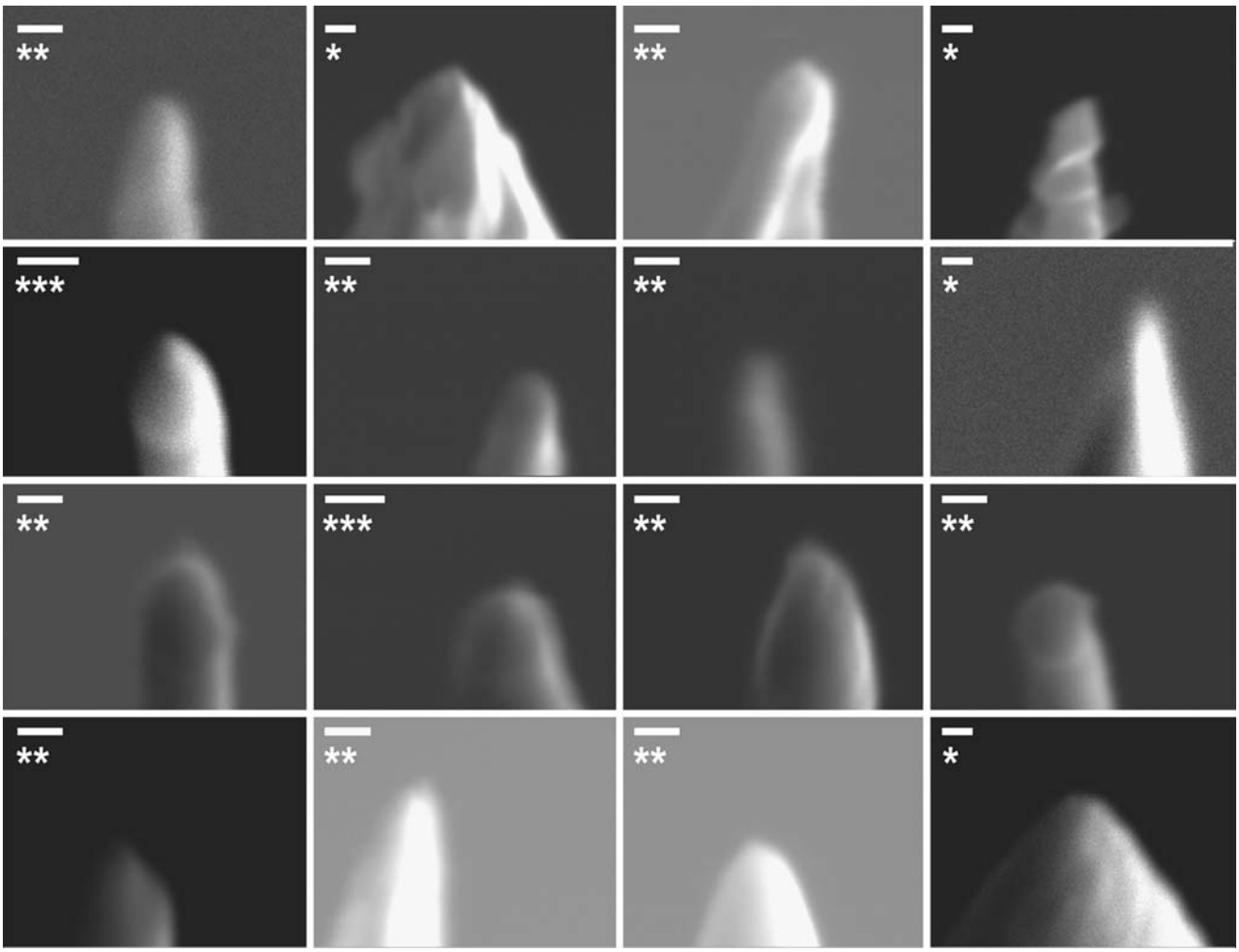

Fig. 7 SEM images of apexes of fabricated nanotips taken at magnifications of *×6K, **×10K, and ***×15K and shown from *left to right* and *up to down* corresponding to the experiments no. 1–16. The *white scale bar* in each subfigure is equal to 1 μm

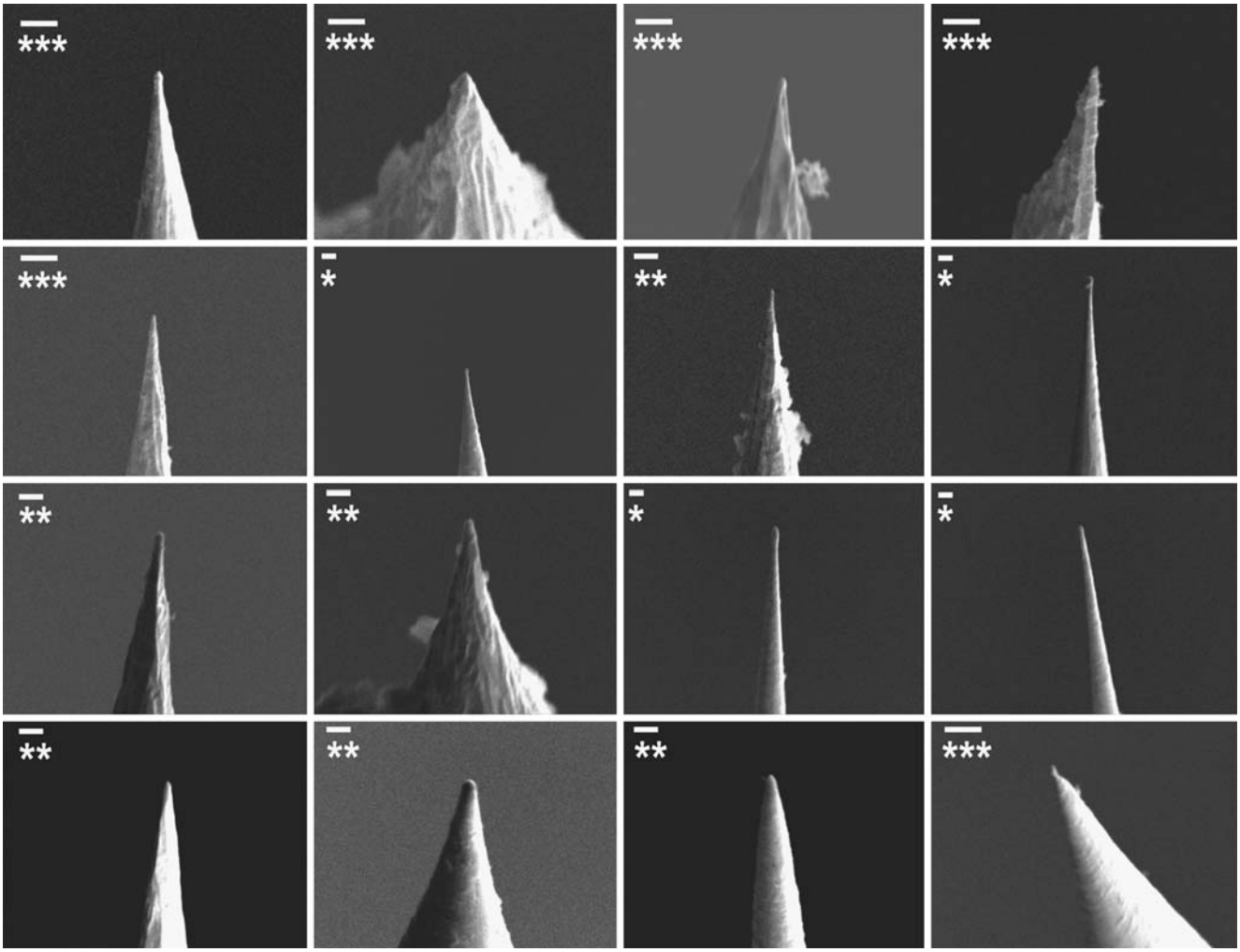

Fig. 8 SEM images of apexes of fabricated nanotips taken at magnifications of *×100K, **×150K, and ***×200K and shown from *left to right* and *up to down* corresponding to the experiments no. 1–16. The *white scale bar* in each subfigure is equal to 100 nm

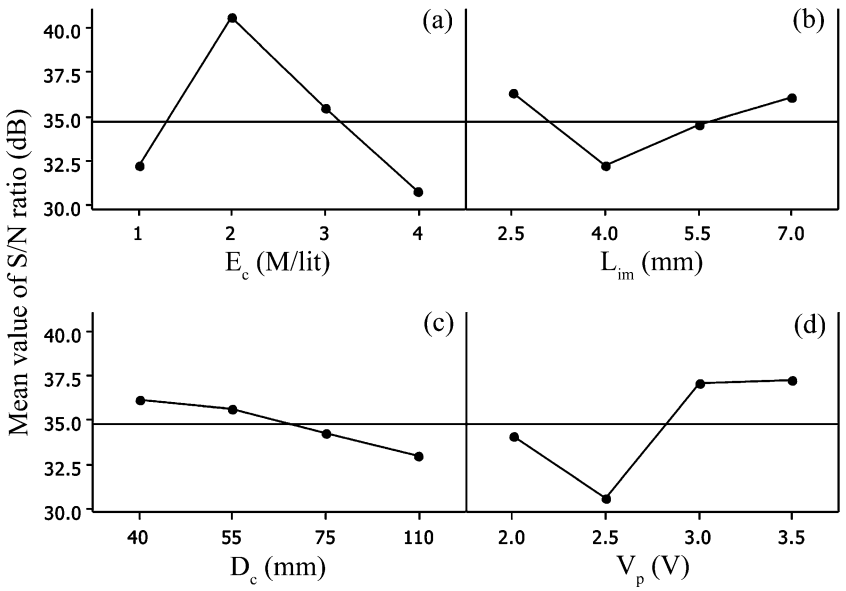

Fig. 9 Effect of different levels of process parameters on S/N ratio: **a** E_c, **b** L_{im}, **c** D_c, and **d** V_p

obtaining optimum level of process parameters. The S/N ratio can be calculated as a logarithmic transformation of the loss function. For HB, the S/N ratio can be expressed as:

$$\eta = -10\log_{10}\left(\frac{1}{n}\sum_{i=1}^{n}\frac{1}{y_i^2}\right) \quad (1)$$

where y_i is the response of the ith experiment and n is the repetition of each experiment. Regardless of the category of the performance characteristic, a larger S/N ratio corresponds to a better performance characteristic. Therefore, the optimum level of the process parameters is the level with the highest S/N ratio. The S/N ratios of L_{16} experiments are shown in Table 1. As an example, the calculation of S/N ratio for experiment no.1 is as follows:

$$\eta = 10\log_{10}\left(\frac{1}{57^2}\right) = 35.1175\text{dB} \quad (2)$$

The mean of S/N ratio values for a process parameter in a defined level is determined by using the S/N ratio values given in Table 1. For example, the mean value of S/N ratios for E_c in level 1 is:

$$\frac{1}{4}(35.1175 + 26.8485 + 32.4650 + 34.3201) = 32.19\text{dB} \quad (3)$$

Figure 9a–d shows the mean value of S/N ratio against different levels of E_c, L_{im}, D_c, and V_P parameters. According to the results shown in Fig. 9, it can be concluded that:

1. Increase of electrolyte concentration (E_c) to 2 M/lit (level 2) improves the nanotip aspect ratio but beyond that, the nanotip aspect ratio decreases. Consequently, the best level of E_c for optimization of the aspect ratio is about 2 M/lit (level 2)
2. At wire immersion length (L_{im}) of 2.5 mm, the nanotip aspect ratio is high. Increase of the immersion length from 2.5 to 4 mm causes decrease of the nanotip aspect ratio. Further, increase of the immersion length causes increase of the nanotip aspect ratio again. The best immersion length seems to be 2.5 mm (level 1)
3. The nanotip aspect ratio decreases inversely, with inner diameter of the cathode tube (D_c). Thus, the best level of D_c for optimization of the aspect ratio is about 40 mm (level 1)

Table 2 Analysis of variance for S/N ratios of nanotip aspect ratio

Source	f	SS	V	F	P_p (%)
E_c	3	229.035	76.345	25.05	54.1
L_{im}	3	41.393	13.798	4.53	9.8
D_c	3	25.161	8.387	2.75	6
V_p	3	118.697	39.566	12.98	28
Error	3	9.144	3.048		2.1
Total	15	423.430			100

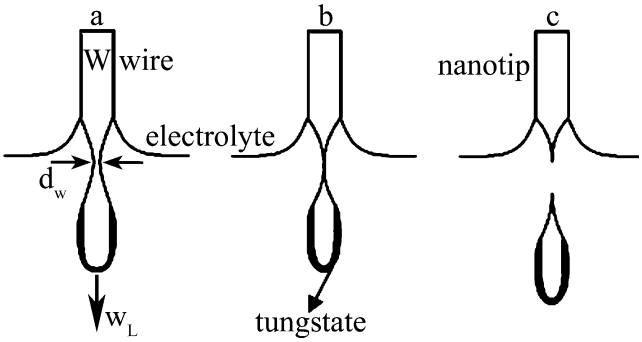

Fig. 10 Sequences of generation of nanotip

4. Increase of the process voltage (V_p) to 2.5 V causes decrease of the nanotip aspect ratio to a minimum. Further process voltage increase gives rise to a better aspect ratio. Therefore, the best level of voltage for optimization of the aspect ratio is about 3.5 V (level 4). Higher voltages can give rise to oxide layer generation on the apex of tip [17]

Based on the mentioned conclusions, it is found that the best combination of E_c, L_{im}, D_c, and V_p levels to achieve optimum aspect ratio of nanotip are 2, 1, 1, and 4, respectively.

4.2 Analysis of variance

The analysis of variance is used to discuss the relative importance of process parameters on the nanotip aspect ratio. The ANOVA is based on the following factors [34]:

- Degree of freedom (f): f denotes the number of independent variables and is calculated as:

$$f_T = N - 1,\quad f_p = L_p - 1,\quad f_e = f_T - \sum f_p \quad (4)$$

  where f_T is the total degree of freedom, N is the total number of experiments, f_p is the degree of freedom for each parameter, L_p is the number of levels for the parameter, and f_e is the degree of freedom for error.
- Sum of squares (SS): SS_T, SS_p, and SS_e denote the total sum of squares, the sum of squares for each parameter, and the sum of squares of the error correlated to all parameters, respectively

$$\begin{aligned} SS_T &= \sum_{i=1}^{m}\eta_i^2 - \frac{1}{m}\left(\sum_{i=1}^{m}\eta_i\right)^2 \\ SS_p &= \frac{1}{n}\sum_{j=1}^{n}(S_{\eta j})^2 - \frac{1}{m}\left(\sum_{i=1}^{m}\eta_i\right)^2 \\ SS_e &= SS_T - \sum SS_p \end{aligned} \quad (5)$$

  where η_i is the S/N ratio of ith experiment, m is the total number of experiments, n is the repetition of each level

Table 3 Results of the confirmation experiment

	Optimum conditions	
	Prediction	Experiment
Level	2, 1, 1, 4	2, 1, 1, 4
S/N Ratio (dB)	46.0337	44.7106

of the parameter, $S_{\eta j}$ is the sum of the S/N ratio involving the parameter and level j (Table 1).

- Variance (V): The variance related to each parameter (V_p) and the variance of error (V_e) is defined as follows:

$$V_p = \frac{SS_p}{f_p}, \quad V_e = \frac{SS_e}{f_e} \tag{6}$$

- F-ratio (F): The F-ratio of each parameter (F_p) is given by

$$F_p = \frac{V_p}{V_e} \tag{7}$$

- Percentage of the contribution (P_p): P_p denotes the percentage of the total variance of each individual parameter

$$P_p(\%) = \frac{SS_p}{SS_T} \times 100 \tag{8}$$

The results obtained from ANOVA of S/N ratios are shown in Table 2. Greater F value and percentage contribution (P_p) for a parameter determine higher impact of the parameter on the nanotip aspect ratio. Considering the ANOVA results given in Table 2, the process parameters can be ranked in terms of their impact on the nanotip aspect ratio as electrolyte concentration, process voltage, wire immersion length, and inner diameter of the cathode tube, respectively.

4.3 Discussion

Figure 10 represents the schematic diagram of the setup for nanotip fabrication. In this figure, d_w is the minimum diameter of the tungsten wire at the necked region and w_L is the weight of the lower part of the wire which breaks down. δL_{nr} is elongation value of the necked region. The d_w and δL_{nr} are a function of etching rate and elongation rate of the necked region. w_L is a function of L_{im}, etching rate of the lower part of the wire, and the amount of the tungstate deposited on the lower part of the wire during the process. The necked region becomes thinner and more lengthened by effect of etching and elongation under load w_L until the lower part of the wire is separated. The sequences of nanotip fabrication can be divided into three stages: (a) before separation of the lower part of the tungsten wire, (b) moment of separation, and (c) after separation.

The sum of effects of these three stages determines the final aspect ratio. The drastically influencing factors on the nanotip aspect ratio (L_t/R_t) in mentioned stages can be summarized as follows:

1. The amount of d_w and δL_{nr} at the end of the first stage; smaller d_w results in smaller R_t and larger δL_{nr} gives rise to larger L_t
2. At the second stage, the mechanism of separation of the last atoms at the necked region is under influence of etching performance. Chemical composition and ion

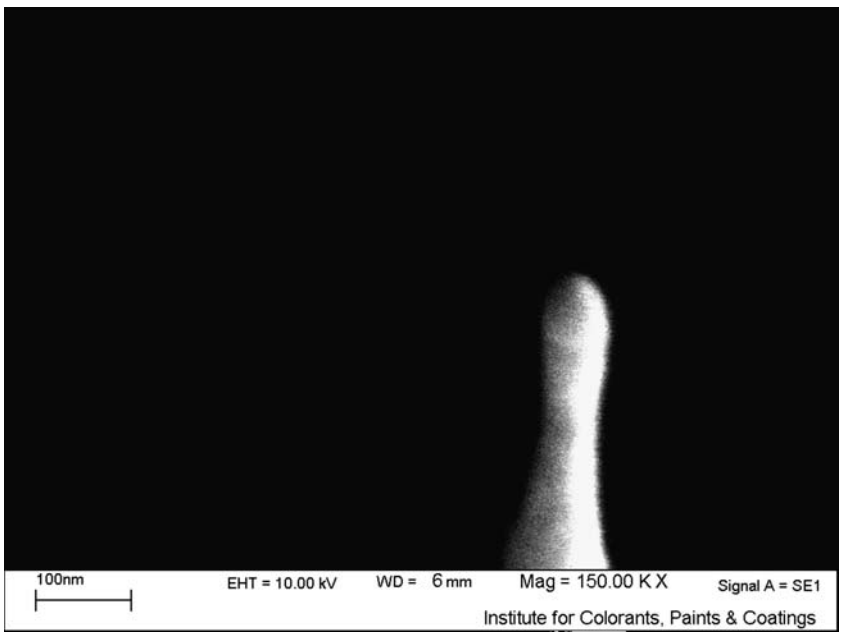

Fig. 11 SEM image of the optimized nanotip taken at ×150K magnification with the apex radius (R_t) of 25 nm approximately

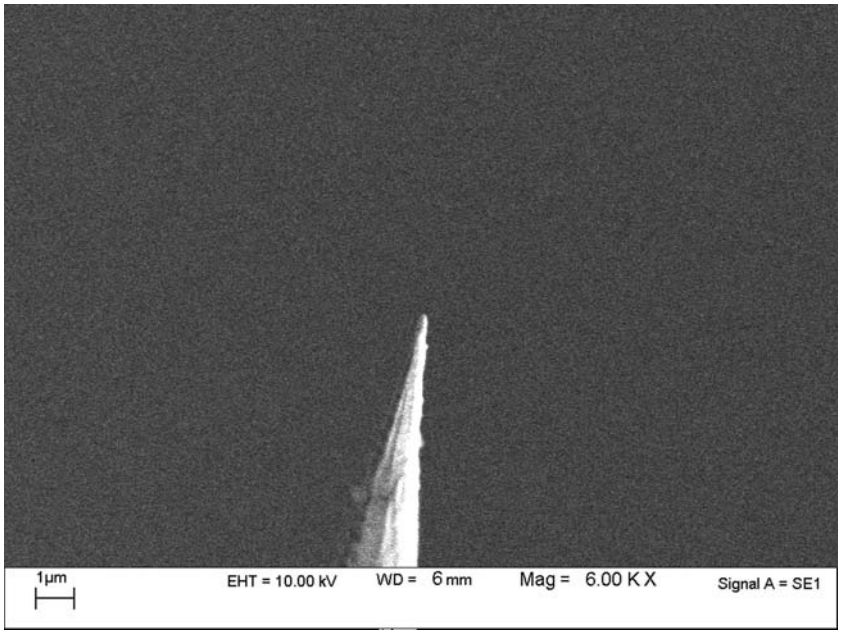

Fig. 12 SEM image of the optimized nanotip taken at ×6K magnification with L_t of 4,300 nm approximately

orientation within the adjacent layers to the neck and physical behavior of the layers like motions within the layers and beyond them, electrical attraction or repulsion of the ions to the necked material, and potential gradient nearby the neck determine the etching performance. Meanwhile, fine separation of the lower part of the wire is affected by proper combination of etching of the necked region and its simultaneous stretching under w_L

3. At the third stage, during time delay in turning off the voltage, the nanotip apex starts to be etched and its aspect ratio and sharpness will decrease. Therefore, the etching rate can affect the nanotip aspect ratio at this stage: the higher the etching rate the lower the aspect ratio

The above-mentioned stages are functions of interaction of etching rate and elongation rate which themselves are dependent upon the E_c, L_{im}, D_c, and V_p.

It seems that, if the etching rate is low, the selective etching from the neck diminishes and the whole body immersed into the electrolyte will be attacked almost uniformly. Therefore, w_L and d_w will decrease almost with the same rate. Consequently, the elongation of the necked

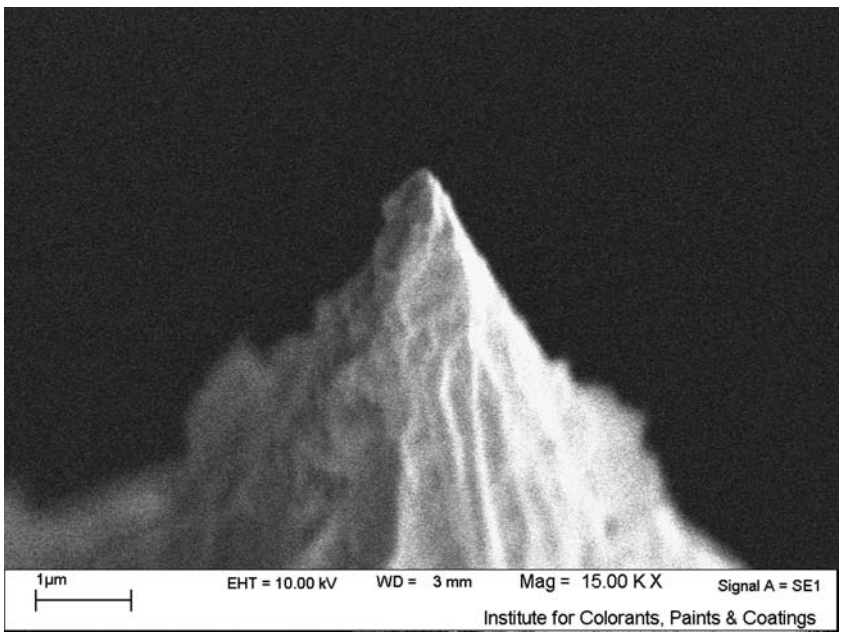

Fig. 13 SEM image of the fabricated nanotip in experiment no. 2

region and reduction of d_w will be low at the first stage. As the lower part and the neck will be etched and removed at the same time, the nanotip aspect ratio will be low. On the other hand, if the etching rate is high the opportunity of elongation of the necked region during the first stage will be low and during the second stage the dominant mechanism of separation will be etching. Consequently, again, the nanotip aspect ratio will be low. If the etching rate of the necked region is in proper interaction with its elongation rate (optimum etching rate), reduction of d_w and elongation of necked region will be high during the first stage. This will provide the necked region to be lengthened further at later stages of etching, leading to separation of the lower part of the wire. This will give rise to high nanotip aspect ratio.

5 Confirmation experiment

In Taguchi method, after the optimum level of the process parameters is determined, the final step is to verify the improvement of the performance characteristic using the optimum level of the process parameters. The estimated S/N ratio (η_{opt}) using the optimum level of the process parameters can be calculated as:

$$\eta_{opt} = \eta_m + \sum_{i=1}^{p} (\overline{\eta_i} - \eta_m) \quad (9)$$

where η_m is the total mean of the S/N ratio (Table 1), p is the number of the process parameters, and $\overline{\eta_i}$ is the mean value of S/N ratio at the optimum level of the parameter. The confirmation experiment was conducted by using the optimum level of the process parameters. The nanotip aspect ratio (L_t/R_t) of 172 (4,300/25 nm) was achieved in this experiment. Table 3 shows the results of the confirmation step. As it is seen, there is a good agreement between the predicted and the actual S/N ratios. The improvement of the S/N ratio was 9.9579 dB and the nanotip aspect ratio was enhanced by 2.63 times in comparison to the mean value of the experimental results shown in Table 1. These results confirmed the capability of the Taguchi method used for optimizing the nanotip aspect ratio. SEM images of optimized nanotip with magnifications of ×150K and ×6K are shown in Figs. 11 and 12, respectively. SEM image of the fabricated nanotip in experiment no. 2 is shown in Fig. 13 for comparison.

6 Conclusion

The most important parameters that govern the nanotip fabrication process of tungsten wire are the time delay in turning off the process voltage, electrolyte concentration, immersion length of the tungsten wire, inner diameter of the cathode tube, and the process voltage. Time delay in turning off the process voltage should be as low as possible. In this research, with design and manufacture of an electronic circuit, this time delay was fixed on 100 ns. For optimization of the nanotip aspect ratio, the effects of other process parameters were studied by using Taguchi method. It was shown that the optimum level of process parameters are electrolyte concentration of 2 M/lit, wire immersion length of 2.5 mm, cathode tube inner diameter of 40 mm, and process voltage of 3.5 V. Based on the ANOVA results, it was shown that the process parameters in terms of impact significance are electrolyte concentration, process voltage, wire immersion length, and inner diameter of the cathode tube. By using the optimum level of the process parameters, the nanotip aspect ratio was enhanced by 263% in comparison to the mean value of the experimental results. The nanotip aspect ratio of 22:1–163:1 was obtained in this study.

References

1. Rangelow IW, Biehl St (2001) High aspect ratio silicon tips field emitter array. Microelectron Eng 57–58:613–619. doi:10.1016/S0167-9317(01)00492-0
2. Pasquini A, Picotto GB, Pisani M (2005) STM carbon nanotube tips fabrication for critical dimension measurements. Sens Actuators A Phys 123–124:655–659. doi:10.1016/j.sna.2005.02.036
3. Vasile MJ, Grigg DA, Griffith JE et al (1991) Scanning probe tips formed by focused ion beams. Rev Sci Instrum 62(9):2167–2171. doi:10.1063/1.1142334
4. Resnik D, Vrtacnik D, Aljancic U et al (2003) Different aspect ratio pyramidal tips obtained by wet etching of (100) and (111) silicon. Microelectron J 34:591–593. doi:10.1016/S0026-2692(03)00056-9
5. Kazinczi R, Szocs E, Ka'lma'n E et al (1998) Novel Methods for Preparing EC-STM tips. Appl Phys A 66:535–538. doi:10.1007/s003390051197
6. Boyle MG, Feng L, Dawson P (2007) Safe fabrication of sharp gold tips for light emission in scanning tunnelling microscopy. Ultramicroscopy 108:558–566. doi:10.1016/j.ultramic.2007.08.012
7. Kerfriden S, Ayssar HN, Campbell SA et al (1998) The electrochemical etching of tungsten STM tips. Electrochim Acta 43:1939–1944. doi:10.1016/S0013-4686(97)00316-2
8. Muller AD, Muller F, Hietschold M et al (1999) Characterization of electrochemically etched tungsten tips for scanning tunneling microscopy. Rev Sci Instrum 70:3970–3972. doi:10.1063/1.1150022
9. Schmidt U, Rasch H, Fries T et al (1992) Characterization of STM W-tips by FIM with an organic image gas. Surf Sci 266:249–252. doi:10.1016/0039-6028(92)91028-A
10. Méndez J, Luna M, Baró AM (1992) Preparation of STM W tips and characterization by FEM, TEM and SEM. Surf Sci 266:294–298. doi:10.1016/0039-6028(92)91036-B
11. Hockett LA, Creager SE (1993) A convenient method for removing surface oxides from tungsten STM tips. Rev Sci Instrum 64:263–264. doi:10.1063/1.1144394

12. Oliva AI, Romero GA, Pena JL et al (1996) Electrochemical preparation of tungsten tips for a scanning tunneling microscope. Rev Sci Instrum 67(5):1917–1921. doi:10.1063/1.1146996
13. Ottaviano L, Lozzi L, Santucci S (2003) Scanning Auger microscopy study of W tips for scanning tunneling microscopy. Rev Sci Instrum 74(7):3368–3378. doi:10.1063/1.1581392
14. Zhang R, Ivey DG (1996) Preparation of sharp polycrystalline tungsten tips for scanning tunneling microscopy imaging. J Vac Sci Technol B 14(1):1–10. doi:10.1116/1.589029
15. Melmed AJ (1991) The Art and science and other aspects of making sharp tips. J Vac Sci Technol B 9:601–608. doi:10.1116/1.585467
16. Lemke H, Goddenhenrich T, Bochem HP et al (1990) Improved microtips for scanning probe microscopy. Rev Sci Instrum 61:2538–2541. doi:10.1063/1.1141911
17. Ibe JP, Bey PP Jr, Brandow SL et al (1990) On the electrochemical etching of tips for scanning tunneling microscopy. J Vac Sci Technol A 8(4):3570–3572. doi:10.1116/1.576509
18. Fainchtein R, Zarriello PR (1992) A computer-controlled technique for electrochemical STM tip fabrication. Ultramicroscopy 42–44:1533–1537. doi:10.1016/0304-3991(92)90478-3
19. Bourque H, Leblanc RM (1995) Electrochemical fabrication of scanning tunneling microscopy tips without an electronic shut-off control. Rev Sci Instrum 66:2695–2697. doi:10.1063/1.1145612
20. Klein M, Schwitzgebel G (1997) An improved lamellae drop-off technique for sharp tip preparation in scanning tunneling microscopy. Rev Sci Instrum 68:3099–3103. doi:10.1063/1.1148249
21. Kar AK, Gangopadhyay S, Mathur BK et al (2000) A reverse electrochemical floating-layer technique of SPM tip preparation. Meas Sci Technol 11:1426–1431. doi:10.1088/0957-0233/11/10/302
22. Nicolaides R, Yong L, Packard WE et al (1988) Scanning tunneling microscope tip structures. J Vac Sci Technol A 6 (2):445–447. doi:10.1116/1.575392
23. Quaade UJ, Oddershede L (2002) Electrochemical etching of sharp tips for STM reveals singularity. Europhys Lett 57(4):611–617. doi:10.1209/epl/i2002-00505-4
24. Greiner M, Kruse P (2007) Recrystallization of tungsten wire for fabrication of sharp and stable nanoprobe and field-emitter tips. Rev Sci Instrum 78(2):026104. doi:10.1063/1.2670293
25. Krakauer BW, Hu JG, Kuo SM et al (1990) A system for systematically preparing atom-probe field-ion-microscope specimens for the study of internal interfaces. Rev Sci Instrum 61:3390–3398. doi:10.1063/1.1141590
26. Krakauer BW, Seidman DN (1992) Systematic procedures for atom-probe field-ion microscopy studies of grain boundary segregation. Rev Sci Instrum 63:4071–4079. doi:10.1063/1.1143214
27. Morgan R (1967) An automatic electropolishing supervisor for preparing field ion microscope specimens. J Sci Instrum 44 (9):808–809. doi:10.1088/0950-7671/44/9/447
28. Chen Y, Xu W, Huang J (1989) A single new technique for preparing STM tips. J Phys E Sci Instrum 22(7):455–457. doi:10.1088/0022-3735/22/7/009
29. Anwei L, Xiaotang H, Wenhui L et al (1997) An improved control technique for the electrochemical fabrication of scanning tunneling microscopy microtips. Rev Sci Instrum 68:3811–3813. doi:10.1063/1.1148032
30. Xu D, Liechti KM, Ravi-Chandar K (2007) Mesoscale scanning probe tips with subnanometer rms roughness. Rev Sci Instrum 78 (7):073707. doi:10.1063/1.2756997
31. Kim P, Jeong S, Jeong MS (2007) Effects of process parameters on the electrochemical etching of sharp metallic tips with an attached mass. Rev Sci Instrum 78(9):096105. doi:10.1063/1.2785851
32. Park J, Park K, Choi B et al (2003) A novel fabrication process for ultra-sharp, high-aspect ratio nano tips using (111) single crystalline silicon. 12th International Conference on Transducers, Solid-State Sensors, Actuators and Microsystems 2, pp 144–1145
33. Tsong TT (1990) Atom-probe field ion microscopy. Cambridge University Press, Cambridge
34. Ross PJ (1989) Taguchi techniques for quality engineering. McGraw-Hill, New York
35. Garcia-Diaz A, Philips DT (1995) Principles of experimental design and analysis. Chapman & Hall, London
36. Montgomery DC (2001) Design and analysis of experiments. Wiley, New York
37. Cox DR, Reid N (2000) The theory of the design of experiments. Chapman & Hall/CRC, London
38. Phadke MS (1989) Quality engineering using robust design. Prentice Hall, Englewood Cliffs, NJ
39. Evans UR (1960) The corrosion and oxidation of metals. Arnold, London